Annual Review of Biophysics

Nanopore Single-Molecule Chemistry

Yao Liu,[1] Xinmeng Gao,[2] and Shuo Huang[2]

[1]Institute of Biomedical Engineering, School of Life Sciences, Suzhou Medical College of Soochow University, Suzhou, China; email: liuyao61@suda.edu.cn

[2]State Key Laboratory of Analytical Chemistry for Life Sciences, School of Chemistry and Chemical Engineering; and Chemistry and Biomedicine Innovation Center (ChemBIC), ChemBioMed Interdisciplinary Research Center, Nanjing University, Nanjing, China; email: shuo.huang@nju.edu.cn

Annu. Rev. Biophys. 2026. 55:277–300

The *Annual Review of Biophysics* is online at biophys.annualreviews.org

https://doi.org/10.1146/annurev-biophys-021424-125106

Keywords

nanopore engineering, single-molecule chemistry, biosensor, hetero-nanopore, machine learning

Abstract

Nanopores have become transformative tools in single-molecule chemical analysis, enabling detailed interrogation of molecular interactions and reaction dynamics. These advancements have revolutionized the characterization of chemical kinetics and stereospecificity, broadening nanopore applications. This review evaluates the principles of nanopore single-molecule chemistry, highlighting breakthroughs in chemically reactive nanopore construction via site-specific mutagenesis, semisynthetic engineering, and orthogonal modifications. Notably, we highlight the innovative strategies enabling precise subunit stoichiometry control to ensure single-molecule reactions, and the integration of machine learning for high-fidelity ionic current analysis. These developments position nanopores as versatile tools for intricate molecular detection in fundamental and applied research. Looking forward, nanopore single-molecule chemistry promises an impact on diagnostics, environmental monitoring, and precision medicine. Integration of molecular dynamics simulations, artificial intelligence–driven protein design frameworks, and microsystems technology may expand detectable species, enhancing robustness and lowering detection limits. Such advancements will deepen our understanding of chemical transformations and support meaningful real-world applications of nanopore technologies.

Contents

1. PRINCIPLES OF NANOPORE SINGLE-MOLECULE CHEMISTRY

In nature, protein channels function as conduits for ions and small molecules across cell membranes. The patch-clamp technique, which emerged in the 1970s as one of the earliest single-molecule methods, enables precise recording and analysis of protein channel activities (50). The combination of these activities has catalyzed the development of nanopore-based single-molecule analysis, an emerging technique employing protein channels and their engineered analogs as nanopore sensors (51). As a versatile tool, nanopores have achieved remarkable progress in chemistry and the life sciences, particularly leveraging their exceptional atomic scale structural reproducibility. The unique label-free and real-time analytical capability of nanopores at the single-molecule level provides critical insights into label-free single-molecule sequencing (15, 16, 29, 32, 53, 66, 122) or sensing of molecules (19, 102, 129).

Nanopore single-molecule chemistry is a distinctive branch in nanopore analysis, characterized by the placement of reactive groups in the pore lumen, directly reporting the formation of chemical bonds with analytes. In this case, a nanopore could be considered a nanoreactor. The binding of a molecule to the reactive group in a nanopore leads to the blockade of the ionic current, manifesting as real-time changes in current, enabling direct observation of single-molecule chemical behavior. This also significantly improves nanopore resolution for small analytes typically undetectable by the conventional size-exclusion mechanism (**Figure 1*a***) (6). By analyzing the amplitude, duration, fluctuation range, and on-off times of each ionic current state, one can observe and analyze in real time the detailed chemical processes (106) (**Figure 1*b***). On the other hand, the ionic current characteristics associated with these single-molecule chemical processes can also serve to identify similar analytes (**Figure 1*c***).

Protein nanopores such as toxins (87, 108), viral pores (126), porins (42, 43, 81), and nuclear pore complexes (2) have highly self-assembled structures with atomically precise and sequence-controlled chemical moieties that can be precisely addressed and manipulated, making them ideal scaffolds as nanoreactors (17, 19, 25, 65). Early in 1995, Finkelstein and colleagues (83) achieved the first real-time observation of covalent bond formation within a nanopore by introducing methanethiosulfonate derivatives into the cysteine-containing diphtheria toxin channel and analyzing the changes in single-channel conductance. The Bayley group (13) engineered four histidine residues into *Staphylococcus aureus* α-hemolysin (αHL) as a reactive domain and observed the

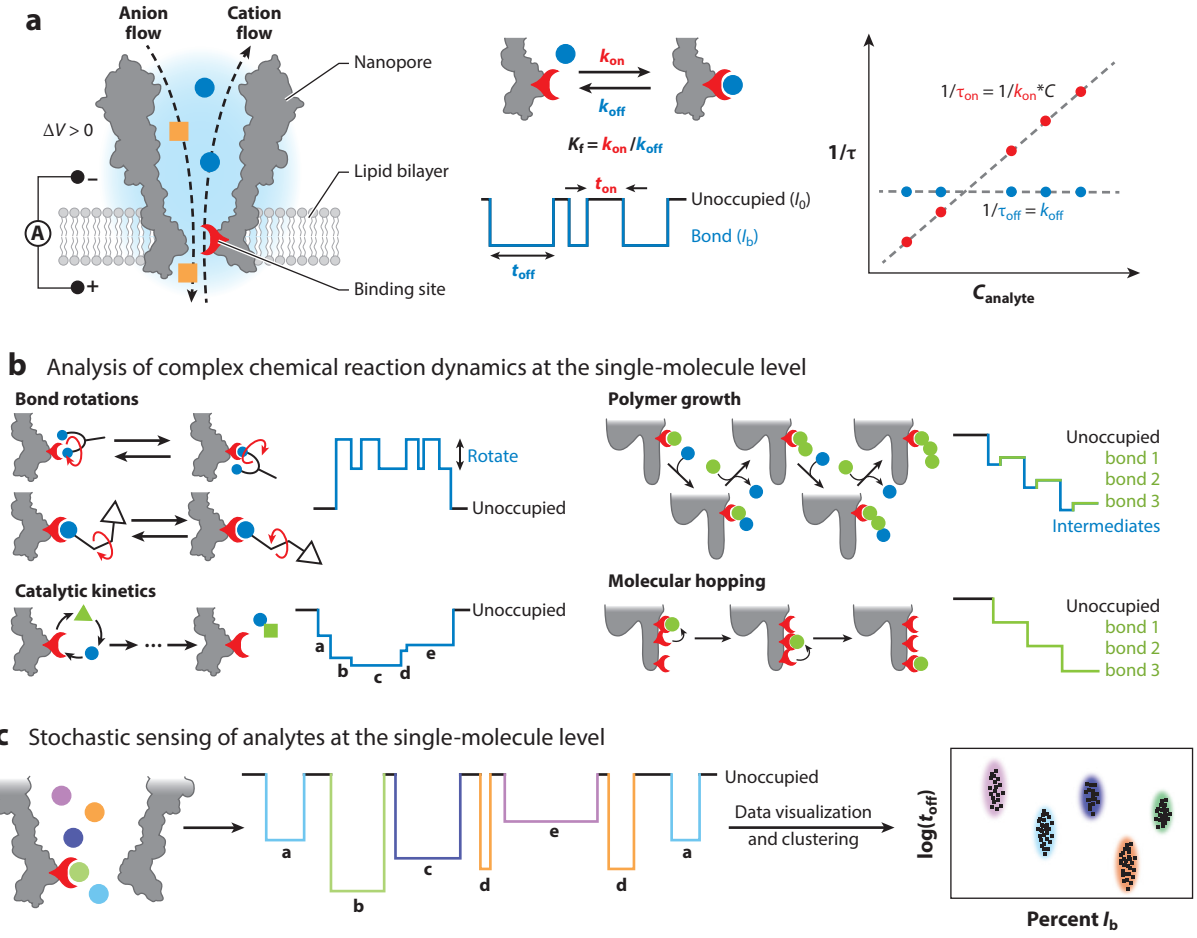

Figure 1

Principles of nanopore single-molecule chemistry. (*a*) Schematic illustration of nanopore observation of single-molecule interactions using a *Mycobacterium smegmatis* porin A (MspA) nanopore. Blue spheres represent target analytes capable of binding to the nanopore's reactive site (*red*), while orange squares denote nontarget analytes lacking complementary binding motifs. Single-molecule association (k_{on}) and dissociation (k_{off}) rate constants can be determined using analyte concentration (C) and fitted values of interevent intervals (τ_{on}) and event dwell times (τ_{off}) extracted from current traces. (*b*) Examples of nanopore single-molecule chemistry measurements. Single-molecule chemical reaction activities, such as bond rotations, catalytic reactions, polymer growth, and molecular hopping, could be directly observed. (*c*) Schematic of stochastic sensing via nanopore single-molecule chemistry. Characteristic events generated by individual analytes exhibit distinct event features, enabling analyte identification.

single-molecule bonding of different divalent metal ions for the first time. These groundbreaking studies demonstrated the early form of nanopore single-molecule chemistry.

In this review, we present the development of nanopore single-molecule chemistry and its applications thereof and highlight how these systems have evolved into highly versatile nanosensors with exceptional spatial and temporal resolution. We illustrate how subtle chemical phenomena, including bond formation, dissociation, isomerization, and molecular interactions, can be monitored using engineered nanopores. Additionally, we discuss the utilization of ionic current signatures generated by different analytes for their identification.

2. INSPIRED BY NATURE: CHEMICAL TAILORING OF PROTEIN NANOPORES

The construction of nanopore single-molecule reactors is target oriented, involving the precise engineering of target-specific reactive groups at predefined sites within the nanopore lumen to enable tailored chemical functions. Over the past two decades, extensive investigations have evolved from substituting natural amino acids to incorporating nonnatural reactive groups via genetic engineering and chemical modification, enabling nanopores to selectively interrogate specific chemical functions (25). A comprehensive overview of these advancements is provided in **Table 1**.

2.1. Introducing Reactive Modules via Site-Specific Mutagenesis

To achieve highly precise and versatile nanopore-based analyses, researchers leverage the intrinsic chemical reactivity of standard amino acid residues, core functional units underpinning protein functionality in biological systems. Functional groups such as the imidazole of histidine, the thiol of cysteine, and amides of asparagine/glutamine are central to ion–molecule interactions, whose collective properties form a versatile toolkit for nanoreactor design. Building on this, site-directed mutagenesis provides a well-established and selective strategy for tailoring protein pores to confer specific sensing functionalities.

The challenge lies in determining where to place such mutation sites. Generally, strategic design at the constriction region of protein nanopores can maximize current fluctuations caused by analyte–nanopore interactions. The Bayley group pioneered the incorporation of functional residues of standard amino acids into nanopores through genetic mutagenesis. As early as 1997, they engineered four histidine residues within the β-barrel structure of αHL, creating a molecular module capable of coordinating divalent metal ions (M^{2+}) one by one (12, 13, 62, 63). Without these engineered sites, the small ionic radius and rapid translocation kinetics of metal ions would hinder clear nanopore-based monitoring. The distinctive signal features generated by these modifications enable differentiation of binding events for Co^{2+}, Zn^{2+}, or Cd^{2+}, facilitating simultaneous stochastic sensing of three ion species. The use of histidine at the constriction of αHL enables high-resolution stochastic sensing of individual metal ions.

The Huang group utilized another pore scaffold, *Mycobacterium smegmatis* porin A (MspA), an octameric, cone-shaped channel protein featuring a uniquely short and narrow constriction zone (≈1.0 nm in length and diameter) for metal ion sensing. This structural property makes single-molecule detection by chemical reaction even easier (37, 81). The M2MspA mutant, optimized by reducing negative charges on its inner surface, has demonstrated exceptional spatial resolution in DNA- and RNA-sequencing applications (18, 31, 67, 82, 84, 85). On the basis of M2MspA, an N91H mutant (MspA-H) was designed for the detection of Co^{2+}, Ni^{2+}, Zn^{2+}, and Pb^{2+} with reproducible ionic current signatures, facilitating parallel comparisons of reaction rate constants (118). The enhanced sensitivity originates from the enhanced electric field at the MspA pore constriction, gained by its unique conical lumen geometry (37, 81).

Mapping potential engineering sites revealed that the spatial resolution inversely correlates with the pore constriction's cross-sectional diameter, identifying residue 91 as the optimal locus for chemical reactivity engineering (137). Substitutions at this site, introducing cysteine, histidine, or aspartic acid (soft, borderline, and hard base functionalities, respectively), enabled selective interactions with Ca^{2+}, Mn^{2+}, Co^{2+}, Ni^{2+}, Zn^{2+}, Pb^{2+}, or Cd^{2+}. These results also validated the hard–soft acid–base principle at the single-molecule scale (118). Replacing Asn91 with methionine (MspA-M) enabled clear observation of reversible binding between thioethers and Au(I)/Au(III) with distinct affinities (20, 21). A single Au^{3+} coordination event in MspA-M produced a current blockage of ∼55 pA, the largest event amplitude caused by a single ion recorded in nanopores to

Table 1 Summary of nanopore-based single-molecule reactors in this review

Strategy	Reactive module	Reaction	Target function	Reference(s)
Mutagenesis	Histidine residue	Coordination with divalent metal ions	Sensing metal ions	12, 13, 62, 63, 118
	Methionine residue	Coordination with Au(I) and Au(III)	Differentiating K_b of Au(III) and Au(I) with thiol	20, 21
	Cysteine residue	Thiol chemistry with methanethiosulfonate derivatives, thioester derivatives, sulfonate ester derivatives, thiol derivatives, organoarsenic(III) compounds, and halogenated acetamide derivatives	Observing formation, rotation, and transfer dynamics of chemical bonds	47, 48, 72, 78, 79, 83, 90, 91, 93, 94, 97, 105, 107, 109
In vitro semisynthesis	Alkyne	CuAAC reactions and oxime chemistry	Observing the formation and dynamics of chemical bonds	68
	Ketone			
	Aromatic residues	CH–π and OH–π interactions with sugars	Stabilizing cyclodextrin adapters in nanopores; differentiating glycans with different aromatic group	69
Genetic code expansion	Azide	Biorthogonal chemistry	Observing in real time the formation and dynamics of chemical bonds	134
	Alkyne			
	Phenyl and amide	Cation–π interactions with peptides	Differentiating mutagenesis in peptides	5, 128
Selective pressure incorporation	Selenocysteine residue	Hydroperoxide reduction by glutathione	Revealing the multicatalytical steps of a seleno-enzyme	59
Chemical modification on cysteine	Phenanthroline-Cu(II) complex	Chelation with amide bonds of norepinephrine, ATP, ADP, D,L-tyrosine, D,L-cysteine, D,L-phenylalanine, D,L-aspartic acid, D,L-tryptophan, and their enantiomers	Sensing neurotransmitters and amino acids	7, 8
	MPBA	Reversible covalent reaction with saccharides, alditols, nucleotide derivatives, salvianolic acid derivatives, and bioacids	Stochastic sensing of *cis*-diols in natural or industrial samples	33, 38–40, 57, 58, 76, 99, 114, 119, 121, 139, 140
	Maleimido-C3-NTA-Ni(II)	Chelation with amide bonds of vitamins, proteinogenic amino acids and their PTMs, and naturally occurring REE(III)s	Stochastic sensing of B vitamins and amino acids and their PTMs in natural samples, and REE(III)s in quartz and bastnaesite	86, 111, 113, 115
	PIDAs	Chelation with Zn(II)	Revealing the main intermediates of the chelation; determining the rate constants of every step	47
	CBT-Mal	Condensation between the CBT and aminothiols	Revealing the structures and lifetimes of the molecules during condensations	95

(*Continued*)

Table 1 (*Continued*)

Strategy	Reactive module	Reaction	Target function	Reference(s)
Chemical modification on histidine	Cu(II)	Chelation with amide bonds of proteinogenic amino acids and phosphorylation/acetylation products	Stochastic sensing of neurotransmitters and amino acids and their PTMs in natural samples	138, 141
	Au(I)	Conversion of acetylenic acids to enol lactones	Revealing catalytic mechanisms of Au(I)	100
Chemical modification on methionine	Oxaziridine reagents with azide/alkyne	CuAAC reaction	Revealing intermediates and mechanistic cycles for the CuAAC reaction	49
	Au(III)	Coordination with cysteine, homocysteine, and GSH	Stochastic sensing of bio-thiols	20

Abbreviations: CBT, 2-cyanobenzothiazole; CBT-Mal, maleimide derivative of CBT; CuAAC, Cu^{+}-catalyzed azide-alkyne cycloaddition; GSH, L-glutathione; MPBA, 3-(maleimide) phenylboronic acid; PIDA, *N*-propyl iminodiacetic acid; PTM, post-translational modification.

date. Additionally, Au^{3+}–thioether coordination served as a bridging motif to sense and discriminate between different biological thiols (20). Engineered MspA mutants can be prepared and purified in parallel without any high-end instruments, as demonstrated in a simplified protocol (131). Excluding the incubation and bacterial culture periods, each variant requires approximately 40 min of manual operation and a material cost of approximately $0.40 to produce a sufficient dose for recording. This cost-efficient workflow facilitates high-throughput screening for novel functionalities, paving the way for broader applications in future single-molecule research.

The scope of sensing residues and analyte targets extends beyond histidine and ions. By introducing reactive cysteine residues derived from functional protein domains into αHL, single-molecule analysis of thiol chemistry becomes feasible. Reactions confined within nanopores represent an ideal model for microscopic biochemical reactions, such as those occurring in enzymatic active sites, offering superior spatial resolution that enables the detection of transient intermediates inaccessible in bulk samples (78). Analytes such as methanethiosulfonate derivatives (83), thioester derivatives (48), sulfonate ester derivatives (133), thiol derivatives (94), organoarsenic(III) compounds (107, 109), and halogenated acetamide derivatives (47, 78, 90) can all report transitions between distinct ionic current states. These state changes reflect either the equilibrium kinetics of covalent interactions with the pore lumen or the bond isomerization within the analyte itself. Quantitatively, the interevent intervals (t_{on}) and blocking event duration times (t_{off}) reflect the kinetics of bond formation and dissociation, respectively. The dissociation constant (k_{off}) can be calculated using $1/\tau_{off} = k_{off}$, while the association constant (k_{on}) can be determined using $1/\tau_{on} = 1/k_{off} {}^{*}C$, where C is the concentration of reactants, and τ is the single exponential fitted value of t (106) (**Figure 1*a***). The kinetics derived from nanopore results are generally consistent with, or slightly higher than, those from other methods (90, 133). The higher kinetics may stem from the increased probability of collisions for bond formation due to nanoconfinement effects. Additionally, inconsistencies in measurement parameters, such as ionic strength, within a nano-confined space often render kinetic results difficult to compare accurately.

An interesting example is the αHL cysteine mutant, within which the reaction of 5,5′-dithiobis(2-nitrobenzoic acid) with the thiol from one bilayer side is followed by cleavage by dithiothreitol from the opposite side. This process triggers pH-dependent cyclization and cysteine regeneration (79). Substituting dithiothreitol with (mercaptoethyl)ether (MEE) inhibits cyclization and instead promotes polymer growth, allowing for detailed characterization of

polymerization kinetics through distinct current signatures (105). Another paradigm involves the reversible interaction between cysteine and 4-sulfophenyl arsonous acid (SPAA) (109). The introduction of L-penicillamine and L-glutathione establishes a Walden cycle network comprising seven molecular states, each associated with a unique current amplitude. Transitions between these states disclose stereochemical principles and thiol exchange kinetics at the arsenic center, exemplifying how nanopores enable nanoscale interrogation of stereoselective bond dynamics. Collectively, these studies highlight the unparalleled capacity of nanopores to resolve intricate molecular mechanisms with single-molecule precision.

Thiol exchange reactions can also occur between closely positioned cysteine residues within a nanopore lumen (48, 72, 91, 93, 94, 97). As engineered by the Bayley group, a cysteine track featuring six thiol groups spaced ∼6 Å in the αHL β-barrel became an innovative single-molecule "walker" model that emulated the directional motion of motor proteins like kinesin. Initially, the organoarsenic(III) compound SPAA–$MEET_2$ was introduced into this cysteine track (91), where reversible As–S bond exchange between adjacent thiols was observed via stochastic current fluctuations. Building on this, Qing et al. (94) designed a disulfide-based molecular hopper comprising a DNA cargo domain and a linear carrier tethered to a streptavidin–biotin complex at one terminus. Under an applied electric field, the DNA cargo exhibited directional movement along the cysteine track, while the carrier anchored the hopper and positioned its reactive disulfide bond at the starting foothold (94). By modulating the carrier's oligomeric state, the disulfide's spatial orientation could be fine-tuned with angstrom-level precision, facilitating investigations of site-selective and regioselective chemistry under nonequilibrium conditions. This molecular hopper functioned as a nanoscale machine capable of "walking" along the cysteine track and discriminating single-nucleotide DNA variations (93, 97), highlighting nanopore platforms as versatile tools for probing complex molecular dynamics and engineering chemically programmable nanodevices.

2.2. Introducing Reactive Modules via Site-Specific Semisynthesis

The rapid advancement of synthetic biology has propelled semisynthetic methodologies such as xenobiology and orthogonal genetic systems (28, 116, 117). By integrating these approaches into biological nanopore reactors through the incorporation of unnatural amino acids (UAAs), researchers can precisely customize chemical reactions while minimizing interference from existing native residues within the pore lumen. Early generations of UAA-substituted nanopores were constructed using solid-phase synthesis (68, 69) and in vitro transcription/translation systems (5), introducing functional moieties like alkynes, ketones, fluorinated phenyl groups, and small aromatic rings into the αHL lumen. These modifications enabled single-molecule-scale observation of Cu^+-catalyzed azide-alkyne cycloaddition (CuAAC), oxime ligation chemistry, and CH–π and OH–π interactions. However, these strategies require robust nanopore self-assembly for structural and functional stability within lipid bilayers, leading to disadvantages such as high costs, low yields, and limited scalability.

Researchers have increasingly employed techniques such as genetic code expansion (128, 134) and selective pressure incorporation (24) to achieve site-specific integration of UAAs during expression. Genetic code expansion utilizes nonsense codons or four-base codons in conjunction with orthogonal tRNA/aminoacyl-tRNA synthetase pairs to control UAA insertion, enabling the incorporation of over 150 distinct UAAs (28). Examples of UAAs integrated into nanopores via genetic code expansion include lysine derivatives like AzK/AlkK (134) and CbzK (128) and phenylalanine derivatives like f5F/Cha/Cpg/Cpa (5), which have been used in single-molecule studies of bioorthogonal chemistry and to probe CH–π interactions. A central challenge in genetic code expansion lies in the screening and engineering of high-fidelity tRNA/aminoacyl-tRNA synthetase pairs to ensure efficient and error-free UAA incorporation. Nevertheless, with optimized systems,

the yield of semisynthetic nanopores has been improved. Breakthroughs include the simultaneous incorporation of up to four distinct UAAs into proteins using genetic code expansion (34) and the development of multisubstrate aminoacyl-tRNA synthetase enzymes compatible with the same *Escherichia coli* host strain (24), thereby expanding the toolkit for tailoring nanopore functionality through UAA integration.

In contrast, selective pressure incorporation employs auxotrophic culture systems and amino acid–deficient host strains to replace a natural amino acid with a structurally analogous UAA, leveraging the substrate compatibility of aminoacyl-tRNA synthetases. For example, Liu and colleagues (59) utilized selective pressure incorporation to introduce selenocysteine into αHL, thereby generating a semisynthetic selenoenzyme nanopore reactor (seleno-αHL). In this approach, a cysteine-auxotrophic *E. coli* strain was cultured in a selenocysteine-supplemented medium, enabling selenocysteine to functionally substitute for cysteine of αHL. This substitution facilitated single-molecule monitoring of glutathione-mediated reduction of hydroperoxides, a multistep reaction involving ultrashort-lived intermediates that are typically inaccessible to conventional techniques. Collectively, these advancements in genetic code expansion and selective pressure incorporation demonstrate powerful methodologies for engineering nanopores with tailored chemical functionalities, thus enabling exploration of complex biochemical pathways at single-molecule resolution.

2.3. Introducing Reactive Modules via Chemical Modification

Beyond genetic engineering, protein channels can be further engineered through chemical modification of amino acid residues to introduce reactive functional moieties temporarily or permanently. For example, functionalizing the Cys117 residue of αHL with a phenanthroline moiety through iodoacetamide conjugation generated a Cu^{2+}-chelated nanopore, which is capable of detecting six neurotransmitters (8) and five pairs of amino acid enantiomers (7). In a different study, Ramsay & Bayley (99) reported that a phenylboronic acid (PBA) adapter was introduced into αHL via thiol-Michael addition. The resulting PBA moiety reversibly forms boronate esters with polyol analytes, enabling direct sensing of D-glucose, D-fructose, and D-maltose. However, according to the statistical results of event dwell time, the discrimination between D-glucose and D-fructose exhibits significant feature overlap, which suggests insufficient pore resolution. This, in turn, may lead to ambiguity in identification. Although discrimination between other sugar isomers or amino acids was also not further reported using these pore configurations, these endeavors established critical design principles for nanopore single-molecule chemical sensors targeting biomolecules such as amino acids, neurotransmitters, and monosaccharides, while also highlighting the potential for further optimizing nanopore systems to enhance the discrimination resolution for structurally similar analytes.

Studies exploring the resolution limits of engineered nanopores have shown that integrating PBA moieties or divalent metal coordination sites into the MspA scaffold can significantly enhance its resolution. In 2022, the Huang group (140) advanced this strategy by constructing a PBA-functionalized nanopore reactor (MspA-PBA), which enabled the detection and discrimination of all nine monosaccharide combinations regardless of their pyranose or furanose conformations in aqueous solution. Concurrently, another study demonstrated that MspA-PBA could resolve all 13 alditol isomers derived from triose, tetrose, and pentose aldoses according to their distinct event features that related to structural differences (76). The outstanding spatial resolution of MspA provides insights into the dynamic formation of boronate esters, with even transient structural changes during chiral boronate ester isomerization manifesting as telegraphic current switching (33). Theoretically, all *cis*-diol-containing biomolecules are viable targets for single-molecule reactions with MspA-PBA, yielding unique current signals. Reported examples include

disaccharide isomers with distinct glycosidic linkages (139); all nucleoside monophosphates (NMPs), diphosphates (NDPs), triphosphates (NTPs), and their major epigenetic modifications (119, 121); nucleotide sugars (114); nucleoside drugs (57); salvianolic acid derivatives (40); and bioacids such as citric, lactic, phenolic, and tartaric acids (38, 39, 58).

The same group developed a Ni-NTA-modified MspA, enabling the first nanopore-based direct differentiation of all 20 proteinogenic amino acids and 4 representative post-translationally modified amino acids (115). This MspA-NTA-Ni platform also efficiently detected five thyroid hormones and seven B vitamins (86, 113). When N_α,N_α-bis(carboxymethyl)-L-lysine hydrate was introduced as a mobile ligand adapter, the system achieved dual-ligand sensing to identify all rare earth elements in a single assay (111). These results all underscore how chemical modification expands the sensing capabilities of MspA across diverse molecular targets.

On the other side, the Huang group in 2020 (118) repurposed the previously published M^{2+}-sensing nanopore (MspA-H) for Cu^{2+} coordination. In this homo-octameric MspA, at the pore constriction, two adjacent histidines and an asparagine from neighboring subunits bind a single Cu^{2+} (138, 141). Despite the facts that homomeric MspA-H-Cu inevitably causes ambiguity in the discrimination between amino acid events and that it shows shorter dwell times and less distinct current fluctuation signatures toward the same analytes compared to MspA-NTA-Ni, this design enabled the detection of three neurotransmitters (141), 20 proteinogenic amino acids, two representative post-translational modifications, and one UAA (138). However, no simultaneous discrimination of all 20 proteinogenic amino acids in the same assay was demonstrated, such that the true discriminatory capacity of this pore was not rigorously validated. The weak affinity between MspA-H and Cu^{2+} would induce spontaneous dissociation of the ion from the pore scaffold, thereby inevitably causing interrupted measurements and ambiguity of event identification, an undesired feature for sequencing applications. To overcome the disadvantages of homomeric nanopores, heteromeric nanopores strictly with a single reactive group to ensure clear observation of single-molecule reactivity, pioneered by the Bayley and Huang groups, have to be applied.

Beyond analyte sensing and discrimination, chemical modification of nanopores enables real-time monitoring of complex reactions with microsecond-scale temporal resolution, allowing for detailed dissection of molecular mechanisms at the single-molecule level (95, 100, 133). For example, covalent attachment of the half-chelator ligand *N*-propyl iminodiacetic acid to αHL revealed key intermediates in the two-step chelation of Zn^{2+} by the bidentate hemichelate assembly. This approach allowed the determination of all relevant major kinetic rate constants (47). Similarly, modification of αHL Cys117 with the maleimide derivative of 2-cyanobenzothiazole (CBT-Mal) enabled characterization of molecular structures and lifetimes during reversible and irreversible condensation reactions between CBT and aminothiols. This method captured transient intermediates such as thioimidate, tetrahedral adducts, and tetrahedral/thiazoline/dihydrothiazine products (95). Chemically functionalized nanopores have also elucidated artificial catalysis mechanisms at the single-molecule level. For instance, coordination of Au(I) to αHL His145 enabled real-time observation of Au(I)-catalyzed conversion of alkynoic acids to enol lactones, disclosing the kinetics of structural rearrangements during catalysis (100). Collectively, these studies highlight the unique capability of chemically modified nanopores to dissect complex chemical and catalytic pathways with exemplary temporal and mechanistic resolution.

In addition to the widely utilized cysteine residues, in situ modification of lysine or methionine offers promising approaches for constructing nanopore reactors. Borsley & Cockroft (10) leveraged reversible iminoboronate chemistry to map the reactivity of αHL lysine residues, demonstrating that modifications to external lysines did not affect the ionic current, whereas those in the constriction region exhibited heightened reactivity. Methionine represents another advantageous target due to its high selectivity toward redox-based modification (49, 70). With the use

of oxaziridine reagents, bioorthogonal azide and alkyne groups were introduced into αHL as first-order reactive modules, enabling subsequent second-order functionalization via click chemistry. This nanopore platform resolved several short-lived intermediates generated during CuAAC.

Notably, while many nanopore teams have investigated reaction intermediates, the current temporal resolution remains inadequate for capturing species with picosecond-scale lifetimes. The Bayley group (96) estimated the upper lifetime limit of such resolvable intermediates to be 80 μs, highlighting a critical constraint. Consequently, improving the capability of nanopores to characterize ultrafast chemical processes, including their transient intermediates, represents a key challenge for the future of nanopore single-molecule chemistry.

3. CONTROLLING THE SUBUNIT STOICHIOMETRY OF NANOPORES TO ENSURE SINGLE-MOLECULE REACTIONS

Except for some single-chain β-barrel transporters like FhuA (35) and OmpG (36), most protein nanopore scaffolds are homomeric (25). Consequently, introducing a target-sensing moiety into any monomeric subunit of the pore would inevitably cause modifications to identical positions across all subunits, forming an undesired ring-shaped reactive domain (**Figure 2*a***), which lacks the control of subunit stoichiometry. From the perspective of the analyte, these moieties are equivalent, often leading to overlapping ionic current signals due to simultaneous interactions (132). Although unreacted modifying molecules may be rapidly removed from the system once a single-site modification succeeds (73), the success probability remains operator dependent and is still technically uncontrollable. Therefore, more stable and reproducible strategies for controlling the number of reactive groups within nanopores are still crucial.

3.1. Heteromeric Transmembrane Pores

The concept of heteromeric transmembrane pores was first introduced in 1997 (13). A hetero-αHL complex containing a subunit with a 4H Zn^{2+}-binding site was synthesized via in vitro transcription/translation and radiolabeled with [^{35}S]methionine (**Figure 2*b*,*f***). In this approach, the 4H monomer and wild-type (WT) monomer were expressed separately, artificially combined at a fixed ratio, and then introduced into rabbit red blood cell membranes or liposomes for assembly. Notably, despite controlled monomer mixing ratios, a diverse array of randomly assembled compositions still emerged. These assemblies were subsequently separated using SDS-PAGE (sodium dodecyl sulfate–polyacrylamide gel electrophoresis) and radiographic imaging and were followed by gel excision and recovery of the $(4H)_1(WT)_6$ hetero-αHL.

Monomers containing sensing groups can also be synthesized via a semisynthetic strategy (68, 69) (**Figure 2*f***). This method involves a three-part construct: A synthetic peptide segment with site-specific, stoichiometrically incorporated alkyne, thiol, or ketone groups is chemically linked between the N-terminal fragment and the C-terminal fragment of αHL. These semisynthetic monomers can assemble in vitro with wild-type monomers to form various hetero-αHL complexes using the same approach. This heteromeric pore strategy has been particularly effective with αHL, primarily due to its ability to form stable monomers after translation, allowing control of in vitro assembly. However, this trait also poses another challenge: Purified hetero-αHL may gradually disassemble over time under environmental fluctuations, reverting to a mixed monomer population. Moreover, many pore-forming proteins exhibit substantially greater stability in their self-assembled oligomeric state than as monomers, making monomer isolation and reassembly difficult. Consequently, in vitro reassembly-based heteromeric pore construction is less suitable for such pores.

Niederweis and colleagues (89) constructed heteromeric pores by fusing all MspA subunits with a peptide linker to create a single-chain MspA containing all eight subunits. Fusion proteins

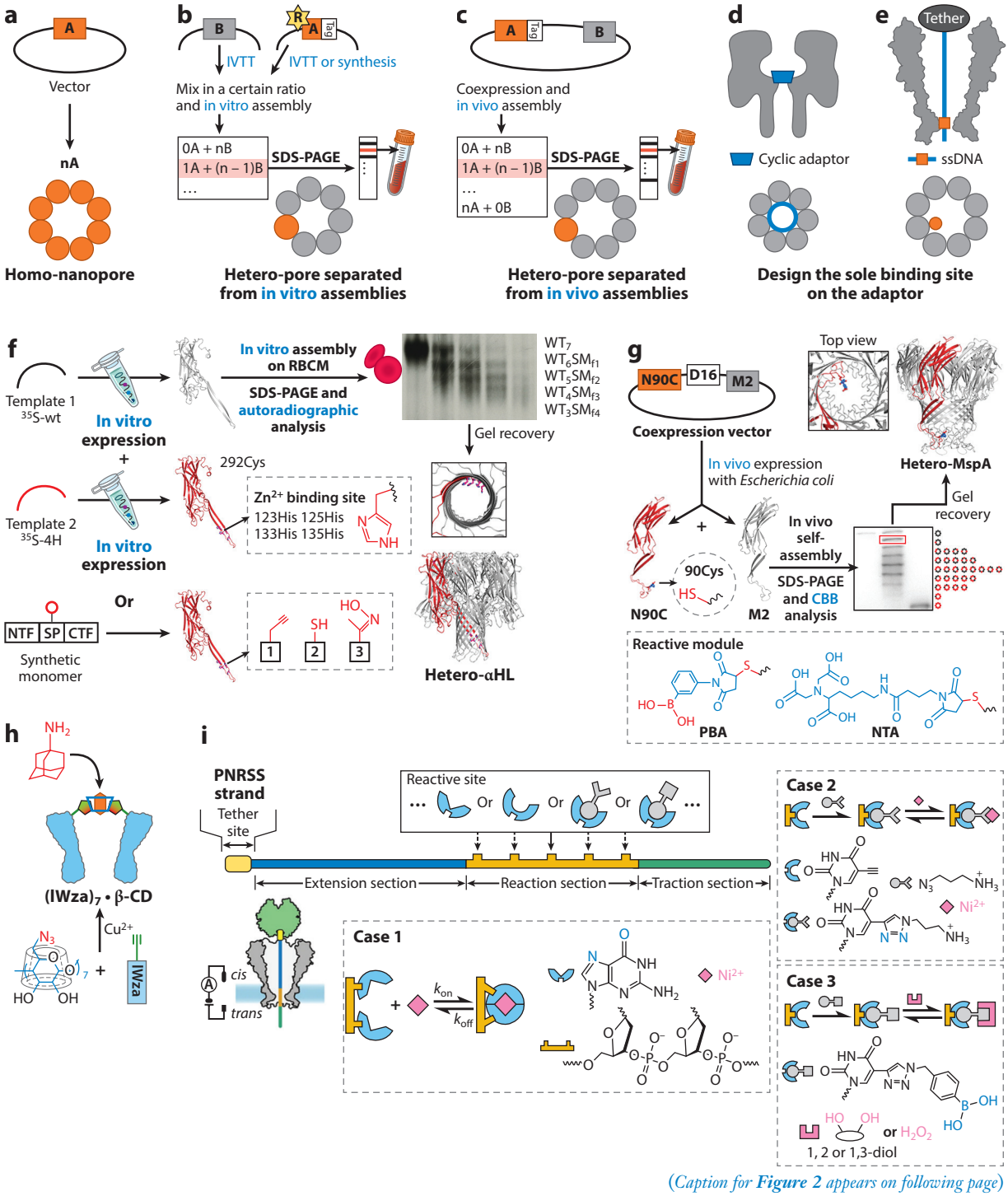

(*Caption for* ***Figure 2*** *appears on following page*)

Figure 2 (*Figure appears on preceding page*)

Strategies to control the subunit stoichiometry of nanopores. (*a–e*) Schematic diagrams illustrating the preparation and structures of homogeneous nanopores (*a*), heterogeneous nanopores (*b*,*c*), and the adaptor-complexed pores (*d*,*e*). Reactive units are shown in orange, while nonreactive units are depicted in gray. Radioactive labels and charged peptide tags, used to assist in separation and purification during electrophoresis, are colored yellow and white, respectively. Adaptors are illustrated in blue. (*f*) Workflow of in vitro fabrication of hetero-nanopores incorporating either in vitro expressed or semisynthetic sensing units. (*g*) Workflow of in vivo preparation of hetero-nanopores. The hetero-nanopore is prepared, assisted by a coexpression vector. Conventional gel recovery methods can be used for purification. (*h*) A cyclic adapter serves as the sole sensor. An azido derivative of β-CD induces the assembly of lWza into a heptameric nanopore for amantadine sensing. (*i*) Scheme of PNRSS. A functional reactive site is intentionally placed on ssDNA instead of the pore. Abbreviations: αHL, α-hemolysin; β-CD, β-cyclodextrin; CBB, Coomassie brilliant blue; CTF, C-terminal fragment; IVTT, in vitro transcription/translation; MspA, *Mycobacterium smegmatis* porin A; NTA, nitrilotriacetic acid; NTF, N-terminal fragment; PBA, phenylboronic acid; PNRSS, programmable nanoreactors for stochastic sensing; rRBCM, rabbit red blood cell membrane; SDS-PAGE, sodium dodecyl sulfate–polyacrylamide gel electrophoresis; ssDNA, single-stranded DNA; wt, wild type. Panel *f* adapted with permission from Reference 13 (CC BY-NC-ND 4.0). Panel *g* adapted with permission from Reference 76; copyright American Chemical Society, and Reference 139. Panel *i* adapted from Reference 55 (CC BY 4.0).

simplify heteromeric nanopore construction by converting multimers into monomers, but in practice, peptide linkers may unpredictably influence the efficiency of pore assembly. In 2011, Pavlenok & Niederweis (88) achieved coexpression of *mspA*, *mspB*, *mspC*, and *mspD* in *M. smegmatis*, and the genes self-assembled into various hetero-oligomeric MspA pores in vivo, just like the natural heteromeric pore NfpAB with sequence homology to MspA (64, 104). These findings suggest that pore-forming proteins with highly stable self-assembled structures inherently exhibit robust fault tolerance, enabling heterogeneous subunit integration during assembly.

Inspired by these findings, Huang and colleagues (140) developed a coexpression vector harboring two mutant *mspA* genes, enabling efficient prokaryotic expression and in vivo assembly of engineered heteromeric nanopores for the first time (**Figure 2*c*,*g***). By introducing an aspartic acid sequence at the C terminus of one mutant gene, they achieved clearer separation of different heteromeric MspA via SDS-PAGE. Owing to its remarkable resistance to denaturation (74), heteromeric MspA retained a stable oligomeric structure even after staining, generating transmembrane ionic currents indistinguishable from those of homomeric MspA produced by conventional methods. The robustness of MspA eliminates the need for radiographic imaging, as target heteromeric MspA bands can be directly recovered from SDS-PAGE gels. Using this approach, the researchers constructed MspA-$(N90C)_1(M2)_7$ heteromeric pores, which enabled site-specific functionalization with a single molecule of either 3-(maleimide)PBA or maleimido-C3-NTA (**Figure 2*g***). The coexpression-based heteromeric pore strategy is ideal for nanopores with highly stable self-assembled structures that are, however, difficult to stay isolated as monomers.

The single-site functionalization ensures that in complex stochastic sensing mixtures, analytes do not interfere with each other, with each ionic current event corresponding to an independent single-molecule chemical reaction. These innovations underscore the potential of heteromeric nanopores for precise single-molecule detection, especially in complex sample environments where resolving individual signals is critical. To date, only MspA and αHL have been engineered into high-efficiency hetero-assemblies with stable sensing performance. Thus, enhancing hetero-assembly efficiency and stability in other nanopore scaffolds represents a key step toward expanding the diversity of nanopore frameworks.

3.2. Design the Sole Binding Site on an Adaptor

In addition to modifying the nanopore, unique reactive moieties may be incorporated into adaptors, molecules designed to interact with analytes in a 1:1 stoichiometric ratio or sized to accommodate only one analyte per nanopore event. Gu, Bayley, and colleagues (44, 45, 46) first

demonstrated that single α-, β-, and γ-cyclodextrins fit within αHL, aligning their molecular six-/seven-/eightfold symmetry axes with the sevenfold symmetry of αHL (**Figure 2*d***). Analytes like promethazine (45), imipramine (45), 2-adamantanamine (127), and lithocholic acid (127) generate distinct single-molecule ionic current blockades through host–guest interactions with β-cyclodextrin inside αHL. Six amine groups were then modified on specific hydroxyl groups of cyclodextrins, which enabled covalent bonding with cysteines of αHL and achieved enhanced spatial resolution in distinguishing more similar molecules like ribonucleoside NMPs and ribonucleoside NDPs (3). Kang and colleagues (110) introduced an alternative approach using azido-derivatives of α-, β-, and γ-cyclodextrins as templates to integrate alkynyl-modified α-helical peptides (lWza) into a nanopore, enabling the observation of supramolecular interactions with 1-amantadine hydrochloride (1-AdNH_2•HCl) (**Figure 2*b***). Other supramolecular host molecules functioning as single-molecule adaptors in nanopores include cyclic peptides (103), cucurbit[6]uril (14), cucurbit[7]uril (142), pillar[5]arene (60), $GaIII_4L_6$ tetrahedral coordination cages (11, 22, 23), and *semiaza*-bambusurils (101). These advancements highlight the versatility of host–adaptor molecules in enhancing nanopore sensing precision and resolving complex single-molecule chemical interactions.

The Huang group (52, 55, 56) introduced an innovative strategy for constructing programmable nanopore single-molecule reactors termed programmable nanoreactors for stochastic sensing (PNRSS) (**Figure 2*e*,*i***). This approach relocates functional reactive moieties to single-stranded DNA (ssDNA), which is easily synthesized and efficiently captured by nanopores, thereby streamlining the fabrication of nanopore-based single-molecule reactors. Reactive sites intentionally placed on the ssDNA chemically engage with analytes within the nanopore, generating characteristic event signatures. The PNRSS chain, a modular ssDNA construct, comprises three functional domains: extension, reaction, and tethering. Reactive groups, such as guanine, adenine, 5-ethynyl-dU-CE phosphoramidite, and PBA, can be precisely incorporated within the reaction domain.

The PNRSS chain is prevented from complete translocation through the nanopore by tethering its extension domain to structures larger than the nanopore aperture, such as streptavidin–biotin complexes or covalent linkages at the nanopore entrance. Under an applied electric field, the tethered PNRSS chain extends fully, ensuring reproducible positioning of reactive moieties within the nanopore lumen. Using this platform, diverse single-molecule reactions have been directly observed, including those involving hydrogen peroxide, metal ions, ethylene glycol, glycerol, lactic acid, vitamins, catecholamine enantiomers, and nucleoside analogs. Critically, the reactive center's functionality can be rapidly refreshed via voltage-controlled reloading of the PNRSS chain, an advantage that enables repetitive detection of irreversible single-molecule reactions, surpassing limitations of reactive moieties covalently integrated into nanopore scaffolds. This programmable, modular strategy highlights the versatility of PNRSS in expanding the repertoire of detectable single-molecule reactions while addressing challenges associated with traditional reactive-site integration approaches.

4. NANOPORE SINGLE-MOLECULE CHEMISTRY FOR RAPID COMPOSITIONAL ANALYSIS

Alongside engineering advancements, nanopores have demonstrated substantial progress in single-molecule chemical analysis. By precisely integrating reactive moieties capable of reversible interactions with specific analytes, these systems enable selective, sensitive, and quantified detection within complex mixtures. Such mixtures may encompass proteins, nucleic acids, polysaccharides and their degradation products, metabolites, pharmaceuticals, environmental pollutants, and even intricate samples like biological fluids, food matrices, or industrial formulations.

In contrast to macroscopic detection methods, nanopore achieves single-molecule detection limits, contingent on sufficient testing duration. For practical applications, the limit of detection is typically defined by the minimum sample concentration required to generate detectable ionic current events within a 10-minute time frame. Notably, preprocessing steps such as enrichment, desalting, or purification are often unnecessary, provided sample components do not compromise the structural integrity of the nanopore or lipid bilayer. This unique capability underpins a broad spectrum of applications, including disease diagnostics, drug development, environmental monitoring, and food safety assessment.

By nanopore-based single-molecule chemical detection, sample components are classified as target analytes, interfering analytes, or noninterfering analytes (38). Only target analytes undergo predefined chemical reactions within the nanopore, yielding optimal resolution, reproducible single-molecule event signatures, and tightly clustered statistical distributions. By applying rigorous data cleaning criteria to recorded events, researchers isolate characteristic current signals of target analytes for downstream analysis. For nanopore systems relying on size-exclusion mechanisms, precise matching of pore dimensions to analyte molecular sizes is critical yet challenging (143). In contrast, engineered nanopores equipped with site-specific reactive modules offer a more robust analytical solution.

We outline six key steps for single-molecule detection in complex samples:

1. Collection: Record continuous raw ionic current traces containing diverse nanopore events.
2. Noise reduction: Enhance the signal-to-noise ratio to distinguish current events from baseline fluctuations.
3. Thresholding: Identify and extract individual nanopore events using, for example, amplitude or duration thresholds.
4. Feature extraction: Derive quantitative features from each event, such as I_b, t_{off}, standard deviation (std), and transition kinetics ($k2_{on}$, $k2_{off}$) between multiple blockage states.
5. Dimensionality reduction and clustering: Perform event clustering and data cleaning to eliminate noise and interfering signals.
6. Identification and quantification: Recognize target analytes and determine their concentrations using reference standards.

Steps 3–6 are pivotal for ensuring analytical efficiency, accuracy, and confidence. Early methodologies relied on real-time visual inspection and manual curation to characterize current events. For step 3, well-defined rectangular events can be extracted using amplitude or duration thresholds, whereas spike-shaped events require additional baseline noise metrics like root-mean-square deviation. In steps 4 and 5, scatterplots of multiple extracted features facilitate combinatory data cleaning. Step 6 traditionally involves comparing event parameters against single-component standards using rate of event appearance frequency–concentration calibration curves. While automation tools such as ADEPT (4), CUSUM (98), MOSAIC (41), and AutoStepfinder (77) have improved feature extraction throughput, manual intervention and potential observer bias remain common in data cleaning workflows.

The advent of machine learning has profoundly transformed signal processing in nanopore research (26, 125, 135). Machine learning methodologies have emerged as indispensable tools for analyzing complex nanopore datasets, driving rapid progress in noise suppression (112), feature extraction (30, 71), data curation, and analyte classification. For example, hidden Markov models enable precise fitting of multiplateau sequencing signals, while learning time-series shapelets algorithms enhance the discrimination of spike-shaped events. In nanopore systems with high signal-to-noise ratios, machine learning significantly elevates the accuracy of data cleaning and analyte classification. Techniques such as dimensionality reduction, clustering, classification, and

regression minimize human intervention, thereby enhancing objectivity, efficiency, and reliability in automated analytical pipelines (26).

Studies by Huang and colleagues (38–40, 57, 58, 76, 86, 111, 113–115, 119, 121, 139, 140) demonstrated an machine learning–aided nanopore sensing workflow for rapid compositional analysis of complex mixtures (**Figure 3**). Briefly, nanopore-based single-molecule reactors were used to independently assay standard samples of target analytes, including sugars, nucleotides, and amino acids, with their characteristic ionic current blockage events recorded as a training dataset. Such independent recordings can be efficiently done with laboratory-customized (130) or commercial multichannel patch-clamp devices with microelectrode arrays [e.g., Nanion's Orbit mini workstations (136)]. Machine learning classification algorithms were then employed to train and validate multiple models in parallel, with the highest-accuracy model selected for predicting and quantifying unknown components in mixed samples. For instance, when current events from standard NMPs and their epigenetic modifications interacting with MspA-PBA sensors are used as a training set, classifiers like support vector machines (SVMs), naive Bayes, and *K*-nearest neighbors were trained in MATLAB, achieving ≥99.6% accuracy. The optimal SVM model was subsequently applied to decomposed RNA samples, enabling automated analysis of mRNA and natural tRNA modifications (121). Similar approaches have been used for peptide digest analysis (115) and hold promise for sequencing innovations, such as exonuclease-based nucleic acid and protein sequencing (9, 92).

For complex matrices like beverages (39, 76), fruits (38), herbal extracts (40), serum (58), dairy, and egg yolk (86), density-based clustering techniques (e.g., DBSCAN) effectively filter out analytes with nonspecific interactions. In a case study using MspA-PBA sensors to analyze *cis*-diols in fruits, Python-implemented DBSCAN refined noise parameters, enabling the identification and quantification of key components: catechin, sorbitol, malic acid, and fructose. Additionally, One-Class SVM in Python detected outlier events, uncovering novel *cis*-diols in RubyRed kiwifruit (38). This approach also facilitates simultaneous identification of diverse *cis*-diols in distilled and fermented alcoholic beverages (39), generating unique molecular barcodes for each sample type that reflect flavor profiles and quality metrics.

Machine learning is rapidly becoming a foundational pillar of nanopore analytics and other single-molecule bioelectronic technologies (54, 73, 124, 138, 143), offering transformative potential for high-sensitivity applications in disease diagnostics, drug discovery, environmental monitoring, and food safety assurance. Nanopore sensing is now evolving from in vitro lipid bilayer systems to in situ cellular environments (141), advancing its readiness for standardized testing and comparative analysis in real-world scenarios.

5. OUTLOOK

Biological nanopores endowed with chemical reactivity have emerged as revolutionary tools for investigating single-molecule chemical kinetics and stereospecificity, offering superior resolution to decode molecular behaviors at the nanoscale. This strategy overcomes intrinsic limitations imposed by size exclusion effects, enabling precise identification of small-molecule analytes. The MspA nanopore reactor, featuring a unique architecture with a broad lumen for analyte capture/accommodation and a narrow constriction zone for superb single-molecule resolution, exemplifies this technological potential. It has been demonstrated that MspA possesses multiscale sensing capabilities, covering macromolecular complexes in their native states like RNAs (120) and proteins (74, 75) down to small organic molecules (**Figure 4*a***). Here we also present proof-of-concept data to show that MspA exhibits exceptional discriminatory resolution and a broad-sensing dynamic range, enabling simultaneous abundance analysis of diverse molecular

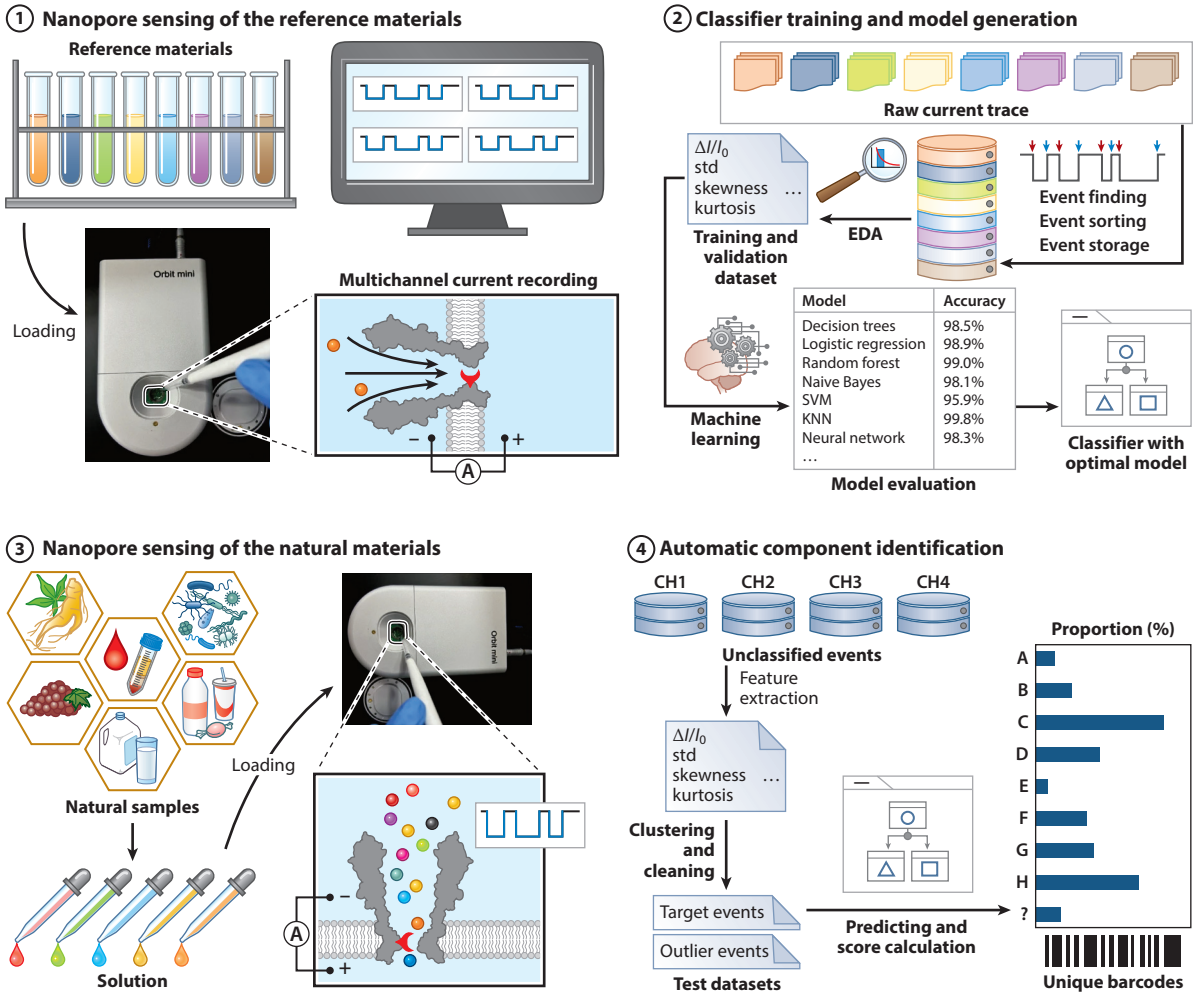

Figure 3

Machine learning–assisted nanopore sensing for rapid compositional analysis of complex mixtures. Step ①: Standard events are first collected through nanopore measurements of reference materials, with event features systematically recorded to facilitate downstream machine learning model development. A commercially available multichannel system, Orbit mini or Orbit 16TC, could be employed to enhance data acquisition efficiency, enabling parallelized sampling and reducing experimental latency. Step ②: Event features, including I_b, t_{off}, std, skewness, and kurtosis, were extracted to construct the training and validation sets. Multiple classification models are then trained in parallel and the optimal model is selected after hyperparameter tuning. Step ③: Under experimental conditions identical to those in step ①, current traces from natural samples are acquired. Step ④: Raw traces are processed using the same feature extraction pipeline defined in step ② to generate an unclassified dataset. Through iterative clustering and outlier detection, target events are separated from spurious signals, yielding refined test sets. The optimized classification model from step ② is then applied to automate component identification, generating a standardized feature barcode that encodes the molecular composition of the sample. Abbreviations: EDA, exploratory data analysis; KNN, *K*-nearest neighbor; std, standard deviation; SVM, support vector machine. The photos of experiment operations in steps ① and ③ were adapted from Reference 38 (CC BY 4.0).

complexes. This includes the analysis of mixtures of protein and oligosaccharide with significant size and molecular weight disparities (**Figure 4*b*,*c***), as well as structurally and chemically distinct yet similarly sized small-molecule analytes such as acids, phenols, saccharides, alcohols, alditols, nucleotides, amino acids, vitamins, and thyroid hormones (**Figure 4*d*,*e***). It is promising

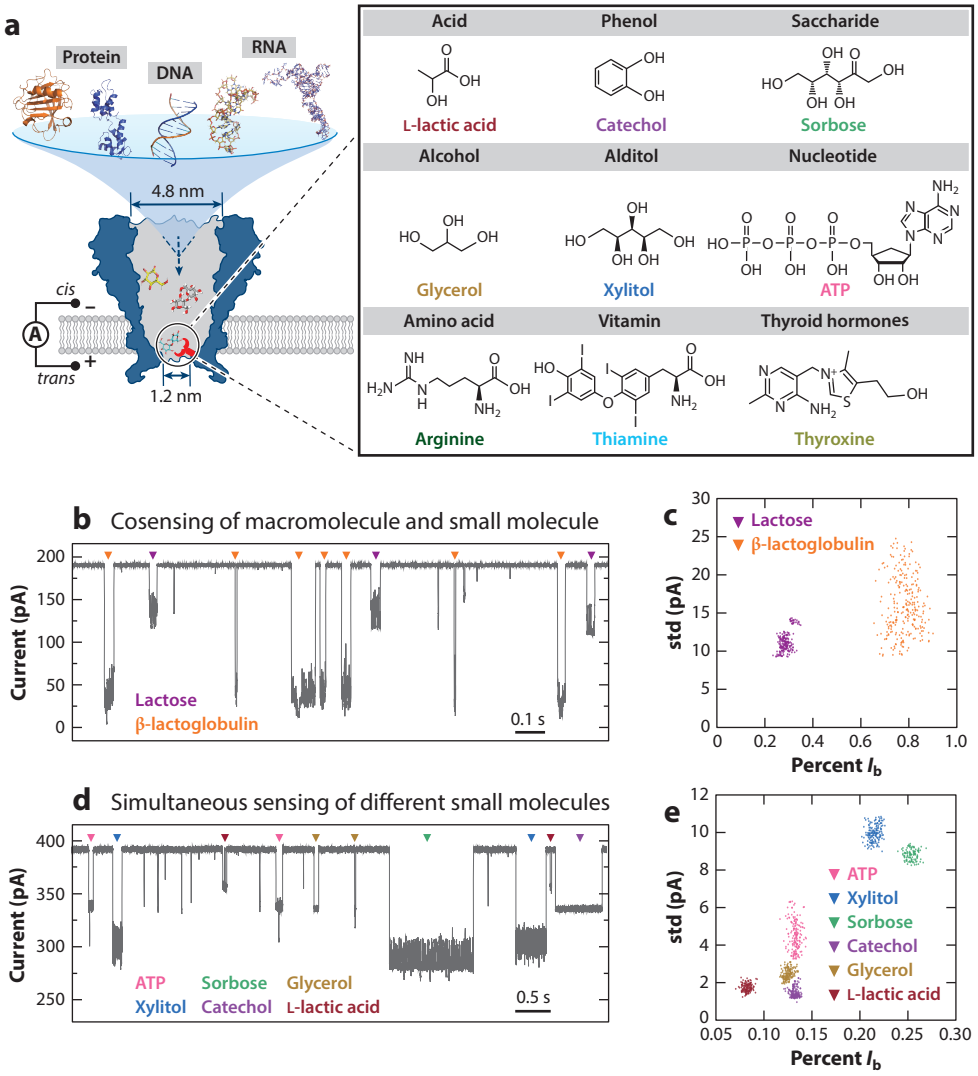

Figure 4

Multifunctional sensing by engineered MspA nanopores. (*a*) Schematic illustration of stochastic sensing of macromolecules and small molecules by engineered MspA. The nanopore's spacious vestibule facilitates accommodation of macromolecules with their native states, whereas its constriction region, equipped with a modular reactive site (*red*), enhances sensitivity for small-molecule sensing. Structures of MspA and representative analytes were generated in PyMOL using PDB IDs 1UUN (MspA), 3BLG (β-lactoglobulin), 1CFC (*apo*-wild-type calmodulin), 1BNA (DNA dodecamer), 2MNC (mRNA), and 1C2X (5S rRNA). The compatible analyte range extends beyond the examples depicted. (*b*) A representative trace obtained upon simultaneous addition of β-lactoglobulin and lactose to the *cis* chamber. Measurements were performed with MspA-PBA in a buffer containing 1.5 M KCl and 100 mM MOPS (pH 7.0) under a continuous transmembrane potential of +80 mV. (*c*) Scatterplot of percentage current blockage (%I_b) versus blocking current std for events extracted from the trace in panel *b*. (*d*) A representative trace acquired with MspA-PBA during simultaneous sensing of ATP, xylitol, sorbose, catechol, glycerol, and L-lactic acid at a +160 mV applied bias. (*e*) Scatterplot of %I_b versus std generated from the events shown in panel *d*. Abbreviations: MOPS, 3-(*N*-morpholino)propanesulfonic acid; MspA, *Mycobacterium smegmatis* porin A; PBA, phenylboronic acid; PDB ID, Protein Data Bank identifier; std, standard deviation.

that nanopores could be functionally partitioned in the future to meet more complex analytical needs, and single-molecule chemical reactivity will undoubtedly be one of the vital capabilities in this regard.

Significant innovative potential remains in optimizing nanopore design and chemical reactivity. Future strategies could focus not only on reactive moieties but also on their surrounding microenvironment to enhance analyte interaction. For instance, molecular dynamics simulations and docking techniques can model behaviors near reactive sites, streamlining design efficiency (61); AI-driven tools, such as AlphaFold for protein structure prediction (1, 27), RFdiffusion for protein backbone generation (123), and transformer-based modeling frameworks (80), may further enable the creation of novel nanopore scaffolds. Coupled with directed evolution, these approaches could greatly expand nanopore diversity. For translational applications, detection throughput and device portability remain key challenges for nanopore-based single-molecule chemical analysis, particularly in field measurements. Although most existing biological nanopores exhibit operational stability for hours or even days during continuous testing, their longevity is often limited by the fragility of phospholipid membranes. Thus, a key priority is the development of robust, easy-to-fabricate materials to replace the fragile lipid bilayers and facilitate device miniaturization. Additionally, the design and manufacture of multichannel nanopore chips, capable of enabling parallel operation of diverse nanopore reactors, could significantly enhance experimental efficiency and reduce detection limits. Integrating microfluidics may further automate sample loading and preliminary purification, improving testing efficiency and reliability across diverse applications.

Data analysis will remain a central pillar of nanopore single-molecule chemistry. The high sensitivity and real-time demands of nanopore technology necessitate ongoing optimization of algorithms and the development of efficient data-processing software. Neural network architectures, such as convolutional neural networks and recurrent neural networks, can be leveraged to develop real-time signal-processing systems for the extraction of critical features and accurate identification of single-molecule events. When integrated with Bayesian analysis frameworks for uncertainty modeling, these AI-driven tools enhance the robustness of signal interpretation in complex environments. In applications like disease diagnostics and real-time monitoring, such high-performance data-processing capabilities will be especially valuable.

In conclusion, the future of nanopore single-molecule chemistry hinges on interdisciplinary collaboration across materials science, molecular biology, and computational science. Innovations in nanopore structural design and data analysis will solidify its role in disease diagnostics, precision medicine, and environmental monitoring. By accelerating technological maturation and adoption, nanopore technology is poised to become a cornerstone for addressing grand challenges in molecular detection.

DISCLOSURE STATEMENT

The authors are not aware of any affiliations, memberships, funding, or financial holdings that might be perceived as affecting the objectivity of this review.

ACKNOWLEDGMENTS

This work was supported by funding from the National Key R&D Program of China (grant 2022YFA1304602), the National Natural Science Foundation of China (grant 22225405), the Fundamental Research Funds for the Central Universities (grant 020514380336) and the State Key Laboratory of Analytical Chemistry for Life Science (grant 5431ZZXM2509).

LITERATURE CITED

1. Abramson J, Adler J, Dunger J, Evans R, Green T, et al. 2024. Accurate structure prediction of biomolecular interactions with AlphaFold 3. *Nature* 630:493–500
2. Ananth AN, Mishra A, Frey S, Dwarkasing A, Versloot R, et al. 2018. Spatial structure of disordered proteins dictates conductance and selectivity in nuclear pore complex mimics. *eLife* 7:e31510
3. Astier Y, Braha O, Bayley H. 2006. Toward single molecule DNA sequencing: direct identification of ribonucleoside and deoxyribonucleoside 5′-monophosphates by using an engineered protein nanopore equipped with a molecular adapter. *J. Am. Chem. Soc.* 128:1705–10
4. Balijepalli A, Ettedgui J, Cornio AT, Robertson JWF, Cheung KP, et al. 2014. Quantifying short-lived events in multistate ionic current measurements. *ACS Nano* 8:1547–53. Erratum. 2015. *ACS Nano* 9:12583
5. Banerjee A, Mikhailova E, Cheley S, Gu L-Q, Montoya M, et al. 2010. Molecular bases of cyclodextrin adapter interactions with engineered protein nanopores. *PNAS* 107:8165–70
6. Bayley H, Cremer PS. 2001. Stochastic sensors inspired by biology. *Nature* 413:226–30
7. Boersma AJ, Bayley H. 2012. Continuous stochastic detection of amino acid enantiomers with a protein nanopore. *Angew. Chem. Int. Ed.* 51:9606–9
8. Boersma AJ, Brain KL, Bayley H. 2012. Real-time stochastic detection of multiple neurotransmitters with a protein nanopore. *ACS Nano* 6:5304–8
9. Bonini A, Sauciuc A, Maglia G. 2024. Engineered nanopores for exopeptidase protein sequencing. *Nat. Methods* 21:16–17
10. Borsley S, Cockroft SL. 2018. In situ synthetic functionalization of a transmembrane protein nanopore. *ACS Nano* 12:786–94
11. Borsley S, Cooper JA, Lusby PJ, Cockroft SL. 2018. Nanopore detection of single-molecule binding within a metallosupramolecular cage. *Chemistry* 24:4542–46
12. Braha O, Gu L-Q, Zhou L, Lu X, Cheley S, Bayley H. 2000. Simultaneous stochastic sensing of divalent metal ions. *Nat. Biotechnol.* 18:1005–7
13. Braha O, Walker B, Cheley S, Kasianowicz JJ, Song L, et al. 1997. Designed protein pores as components for biosensors. *Chem. Biol.* 4:497–505
14. Braha O, Webb J, Gu L-Q, Kim K, Bayley H. 2005. Carriers versus adapters in stochastic sensing. *ChemPhysChem* 6:889–92
15. Branton D, Deamer DW, Marziali A, Bayley H, Benner SA, et al. 2008. The potential and challenges of nanopore sequencing. *Nat. Biotechnol.* 26:1146–53
16. Brinkerhoff H, Kang ASW, Liu J, Aksimentiev A, Dekker C. 2021. Multiple rereads of single proteins at single-amino acid resolution using nanopores. *Science* 374:1509–13
17. Burns JR, Stulz E, Howorka S. 2013. Self-assembled DNA nanopores that span lipid bilayers. *Nano Lett.* 13:2351–56
18. Butler TZ, Pavlenok M, Derrington IM, Niederweis M, Gundlach JH. 2008. Single-molecule DNA detection with an engineered MspA protein nanopore. *PNAS* 105:20647–52
19. Cao C, Long Y-T. 2018. Biological nanopores: confined spaces for electrochemical single-molecule analysis. *Acc. Chem. Res.* 51:331–41
20. Cao J, Jia W, Zhang J, Xu X, Yan S, et al. 2019. Giant single molecule chemistry events observed from a tetrachloroaurate(III) embedded *Mycobacterium smegmatis* porin A nanopore. *Nat. Commun.* 10:5668
21. Cao J, Zhang S, Zhang J, Wang S, Jia W, et al. 2021. A single-molecule observation of dichloroaurate(I) binding to an engineered *Mycobacterium smegmatis* porin A (MspA) nanopore. *Anal. Chem.* 93:1529–36
22. Caulder DL, Powers RE, Parac TN, Raymond KN. 1998. The self-assembly of a predesigned tetrahedral M4L6 supramolecular cluster. *Angew. Chem. Int. Ed.* 37:1840–43
23. Cooper JA, Borsley S, Lusby PJ, Cockroft SL. 2017. Discrimination of supramolecular chirality using a protein nanopore. *Chem. Sci.* 8:5005–9
24. Costello A, Peterson AA, Lanster DL, Li Z, Carver GD, Badran AH. 2024. Efficient genetic code expansion without host genome modifications. *Nat. Biotechnol.* 43:1116–27
25. Crnković A, Srnko M, Anderluh G. 2021. Biological nanopores: engineering on demand. *Life* 11:27

26. Cui F, Yue Y, Zhang Y, Zhang Z, Zhou HS. 2020. Advancing biosensors with machine learning. *ACS Sens.* 5:3346–64
27. Dauparas J, Anishchenko I, Bennett N, Bai H, Ragotte RJ, et al. 2022. Robust deep learning–based protein sequence design using ProteinMPNN. *Science* 378:49–56
28. Davis L, Chin JW. 2012. Designer proteins: applications of genetic code expansion in cell biology. *Nat. Rev. Mol. Cell Biol.* 13:168–82
29. Deamer D, Akeson M, Branton D. 2016. Three decades of nanopore sequencing. *Nat. Biotechnol.* 34:518–24
30. Dematties D, Wen C, Pérez MD, Zhou D, Zhang S-L. 2021. Deep learning of nanopore sensing signals using a bi-path network. *ACS Nano* 15:14419–29
31. Derrington IM, Butler TZ, Collins MD, Manrao E, Pavlenok M, et al. 2010. Nanopore DNA sequencing with MspA. *PNAS* 107:16060–65
32. Dorey A, Howorka S. 2024. Nanopore DNA sequencing technologies and their applications towards single-molecule proteomics. *Nat. Chem.* 16:314–34
33. Du X, Zhang S, Wang L, Wang Y, Fan P, et al. 2023. Single-molecule interconversion between chiral configurations of boronate esters observed in a nanoreactor. *ACS Nano* 17:2881–92
34. Dunkelmann DL, Oehm SB, Beattie AT, Chin JW. 2021. A 68-codon genetic code to incorporate four distinct noncanonical amino acids enabled by automated orthogonal mRNA design. *Nat. Chem.* 13:1110–17
35. Fahie M, Chisholm C, Chen M. 2015. Resolved single-molecule detection of individual species within a mixture of anti-biotin antibodies using an engineered monomeric nanopore. *ACS Nano* 9:1089–98
36. Fahie MA, Chen M. 2015. Electrostatic interactions between OmpG nanopore and analyte protein surface can distinguish between glycosylated isoforms. *J. Phys. Chem. B* 119:10198–206
37. Faller M, Niederweis M, Schulz GE. 2004. The structure of a mycobacterial outer-membrane channel. *Science* 303:1189–92
38. Fan P, Cao Z, Zhang S, Wang Y, Xiao Y, et al. 2024. Nanopore analysis of *cis*-diols in fruits. *Nat. Commun.* 15:1969
39. Fan P, Li K, Li T, Zhang P, Huang S. 2025. Nanopore signatures of major alcoholic beverages. *Matter* 8:101931
40. Fan P, Zhang S, Wang Y, Li T, Zhang H, et al. 2024. Nanopore analysis of salvianolic acids in herbal medicines. *Nat. Commun.* 15:1970
41. Forstater JH, Briggs K, Robertson JWF, Ettedgui J, Marie-Rose O, et al. 2016. MOSAIC: a modular single-molecule analysis interface for decoding multistate nanopore data. *Anal. Chem.* 88:11900–7
42. Fu D, Libson A, Miercke LJW, Weitzman C, Nollert P, et al. 2000. Structure of a glycerol-conducting channel and the basis for its selectivity. *Science* 290:481–86
43. Goyal P, Krasteva PV, Van Gerven N, Gubellini F, Van den Broeck I, et al. 2014. Structural and mechanistic insights into the bacterial amyloid secretion channel CsgG. *Nature* 516:250–53
44. Gu L-Q, Bayley H. 2000. Interaction of the noncovalent molecular adapter, β-cyclodextrin, with the staphylococcal α-hemolysin pore. *Biophys. J.* 79:1967–75
45. Gu L-Q, Braha O, Conlan S, Cheley S, Bayley H. 1999. Stochastic sensing of organic analytes by a pore-forming protein containing a molecular adapter. *Nature* 398:686–90
46. Gu L-Q, Cheley S, Bayley H. 2003. Electroosmotic enhancement of the binding of a neutral molecule to a transmembrane pore. *PNAS* 100:15498–503
47. Hammerstein AF, Shin S-H, Bayley H. 2010. Single-molecule kinetics of two-step divalent cation chelation. *Angew. Chem. Int. Ed.* 49:5085–90
48. Haque F, Lunn J, Fang H, Smithrud D, Guo P. 2012. Real-time sensing and discrimination of single chemicals using the channel of phi29 DNA packaging nanomotor. *ACS Nano* 6:3251–61
49. Haugland MM, Borsley S, Cairns-Gibson DF, Elmi A, Cockroft SL. 2019. Synthetically diversified protein nanopores: resolving click reaction mechanisms. *ACS Nano* 13:4101–10
50. Hladky SB, Haydon DA. 1970. Discreteness of conductance change in bimolecular lipid membranes in the presence of certain antibiotics. *Nature* 225:451–53
51. Howorka S, Siwy Z. 2009. Nanopore analytics: sensing of single molecules. *Chem. Soc. Rev.* 38:2360–84

52. Hu C, Jia W, Liu Y, Wang Y, Zhang P, et al. 2022. Single-molecule sensing of acidic catecholamine metabolites using a programmable nanopore. *Chemistry* 28:e202201033
53. Huang S. 2014. Nanopore-based sensing devices and applications to genome sequencing: a brief history and the missing pieces. *Chin. Sci. Bull.* 59:4918–28
54. Jena MK, Pathak B. 2023. Development of an artificially intelligent nanopore for high-throughput DNA sequencing with a machine-learning-aided quantum-tunneling approach. *Nano Lett.* 23:2511–21
55. Jia W, Hu C, Wang Y, Gu Y, Qian G, et al. 2021. Programmable nano-reactors for stochastic sensing. *Nat. Commun.* 12:5811
56. Jia W, Hu C, Wang Y, Liu Y, Wang L, et al. 2022. Identification of single-molecule catecholamine enantiomers using a programmable nanopore. *ACS Nano* 16:6615–24
57. Jia W, Ouyang Y, Zhang S, Du X, Zhang P, Huang S. 2023. Nanopore signatures of nucleoside drugs. *Nano Lett.* 23:9437–44
58. Jia W, Ouyang Y, Zhang S, Zhang P, Huang S. 2024. Nanopore identification of l-, d-lactic acids, d-glucose and gluconic acid in the serum of human and animals. *Small Methods* 9:e2400664
59. Jiang X, Pan T, Lang C, Zeng C, Hou J, et al. 2022. Single-molecule observation of selenoenzyme intermediates in a semisynthetic seleno-α-hemolysin nanoreactor. *Anal. Chem.* 94:8433–40
60. Jiang X, Zang M, Li F, Hou C, Luo Q, et al. 2021. Highly sensitive detection of paraquat with pillar[5]arenes as an aptamer in an α-hemolysin nanopore. *Mater. Chem. Front.* 5:7032–40
61. Jing B, Stärk H, Jaakkola T, Berger B. 2024. Generative modeling of molecular dynamics trajectories. Preprint, arXiv:2409.17808v1 [q-bio.BM]
62. Kasianowicz J, Walker B, Krishnasastry M, Bayley H. 1993. Genetically engineered pores as metal ion biosensors. *MRS Proc.* 330:217–23
63. Kasianowicz JJ, Burden DL, Han LC, Cheley S, Bayley H. 1999. Genetically engineered metal ion binding sites on the outside of a channel's transmembrane β-barrel. *Biophys. J.* 76:837–45
64. Kläckta C, Knörzer P, Rieß F, Benz R. 2011. Hetero-oligomeric cell wall channels (porins) of *Nocardia farcinica*. *Biochim. Biophys. Acta Biomembr.* 1808:1601–10
65. Langecker M, Arnaut V, Martin TG, List J, Renner S, et al. 2012. Synthetic lipid membrane channels formed by designed DNA nanostructures. *Science* 338:932–36
66. Laszlo AH, Derrington IM, Gundlach JH. 2016. MspA nanopore as a single-molecule tool: from sequencing to SPRNT. *Methods* 105:75–89
67. Laszlo AH, Derrington IM, Ross BC, Brinkerhoff H, Adey A, et al. 2014. Decoding long nanopore sequencing reads of natural DNA. *Nat. Biotechnol.* 32:829–33
68. Lee J, Bayley H. 2015. Semisynthetic protein nanoreactor for single-molecule chemistry. *PNAS* 112:13768–73
69. Lee J, Boersma AJ, Boudreau MA, Cheley S, Daltrop O, et al. 2016. Semisynthetic nanoreactor for reversible single-molecule covalent chemistry. *ACS Nano* 10:8843–50
70. Lin S, Yang X, Jia S, Weeks AM, Hornsby M, et al. 2017. Redox-based reagents for chemoselective methionine bioconjugation. *Science* 355:597–602
71. Liu Q, Fang L, Yu G, Wang D, Xiao C-L, Wang K. 2019. Detection of DNA base modifications by deep recurrent neural network on Oxford Nanopore sequencing data. *Nat. Commun.* 10:2449
72. Liu W, Yang Z-L, Yang C-N, Ying Y-L, Long Y-T. 2022. Profiling single-molecule reaction kinetics under nanopore confinement. *Chem. Sci.* 13:4109–14
73. Liu W, Zhu Q, Yang C-N, Fu Y-H, Zhang J-C, et al. 2024. Single-molecule sensing inside stereo- and regio-defined hetero-nanopores. *Nat. Nanotechnol.* 19:1693–701
74. Liu Y, Pan T, Wang K, Wang Y, Yan S, et al. 2021. Allosteric switching of calmodulin in a *Mycobacterium smegmatis* porin A (MspA) nanopore-trap. *Angew. Chem. Int. Ed.* 60:23863–70
75. Liu Y, Wang K, Wang Y, Wang L, Yan S, et al. 2022. Machine learning assisted simultaneous structural profiling of differently charged proteins in a *Mycobacterium smegmatis* porin A (MspA) electroosmotic trap. *J. Am. Chem. Soc.* 144:757–68
76. Liu Y, Zhang S, Wang Y, Wang L, Cao Z, et al. 2022. Nanopore identification of alditol epimers and their application in rapid analysis of alditol-containing drinks and healthcare products. *J. Am. Chem. Soc.* 144:13717–28

77. Loeff L, Kerssemakers JWJ, Joo C, Dekker C. 2021. *AutoStepfinder*: a fast and automated step detection method for single-molecule analysis. *Patterns* 2:100256
78. Luchian T, Shin S-H, Bayley H. 2003. Kinetics of a three-step reaction observed at the single-molecule level. *Angew. Chem. Int. Ed.* 42:1926–29
79. Luchian T, Shin S-H, Bayley H. 2003. Single-molecule covalent chemistry with spatially separated reactants. *Angew. Chem. Int. Ed.* 42:3766–71
80. Madani A, Krause B, Greene ER, Subramanian S, Mohr BP, et al. 2023. Large language models generate functional protein sequences across diverse families. *Nat. Biotechnol.* 41:1099–106
81. Mahfoud M, Sukumaran S, Hülsmann P, Grieger K, Niederweis M. 2006. Topology of the porin MspA in the outer membrane of *Mycobacterium smegmatis*. *J. Biol. Chem.* 281:5908–15
82. Manrao EA, Derrington IM, Laszlo AH, Langford KW, Hopper MK, et al. 2012. Reading DNA at single-nucleotide resolution with a mutant MspA nanopore and phi29 DNA polymerase. *Nat. Biotechnol.* 30:349–53
83. Mindell JA, Zhan HJ, Huynh PD, Collier RJ, Finkelstein A. 1994. Reaction of diphtheria toxin channels with sulfhydryl-specific reagents: observation of chemical-reactions at the single-molecule level. *PNAS* 91:5272–76
84. Noakes MT, Brinkerhoff H, Laszlo AH, Derrington IM, Langford KW, et al. 2019. Increasing the accuracy of nanopore DNA sequencing using a time-varying cross membrane voltage. *Nat. Biotechnol.* 37:651–56
85. Nova IC, Ritmejeris J, Brinkerhoff H, Koenig TJR, Gundlach JH, Dekker C. 2023. Detection of phosphorylation post-translational modifications along single peptides with nanopores. *Nat. Biotechnol.* 42:710–14
86. Ouyang Y, Wang K, Jia W, Zhang P, Huang S. 2024. Simultaneous identification of vitamins B1, B3, B5, and B6 by an engineered nanopore. *Nano Lett.* 24:11944–53
87. Pastoriza-Gallego M, Rabah L, Gibrat G, Thiebot B, van der Goot FG, et al. 2011. Dynamics of unfolded protein transport through an aerolysin pore. *J. Am. Chem. Soc.* 133:2923–31
88. Pavlenok M, Niederweis M. 2016. Hetero-oligomeric MspA pores in *Mycobacterium smegmatis*. *FEMS Microbiol. Lett.* 363:fnw046
89. Pavlenok M, Yu L, Herrmann D, Wanunu M, Niederweis M. 2022. Control of subunit stoichiometry in single-chain MspA nanopores. *Biophys. J.* 121:742–54
90. Pulcu GS, Galenkamp NS, Qing Y, Gasparini G, Mikhailova E, et al. 2019. Single-molecule kinetics of growth and degradation of cell-penetrating poly(disulfide)s. *J. Am. Chem. Soc.* 141:12444–47
91. Pulcu GS, Mikhailova E, Choi LS, Bayley H. 2015. Continuous observation of the stochastic motion of an individual small-molecule walker. *Nat. Nanotechnol.* 10:76–83
92. Punthambaker S. 2022. Detection of modified RNA with an engineered nanopore. *Nat. Nanotechnol.* 17:1044–45
93. Qing Y, Bayley H. 2021. Enzymeless DNA base identification by chemical stepping in a nanopore. *J. Am. Chem. Soc.* 143:18181–87
94. Qing Y, Ionescu SA, Pulcu GS, Bayley H. 2018. Directional control of a processive molecular hopper. *Science* 361:908–12
95. Qing Y, Liu MD, Hartmann D, Zhou L, Ramsay WJ, Bayley H. 2020. Single-molecule observation of intermediates in bioorthogonal 2-cyanobenzothiazole chemistry. *Angew. Chem. Int. Ed.* 59:15711–16
96. Qing Y, Pulcu GS, Bell NAW, Bayley H. 2018. Bioorthogonal cycloadditions with sub-millisecond intermediates. *Angew. Chem. Int. Ed.* 57:1218–21
97. Qing Y, Tamagaki-Asahina H, Ionescu SA, Liu MD, Bayley H. 2019. Catalytic site-selective substrate processing within a tubular nanoreactor. *Nat. Nanotechnol.* 14:1135–42
98. Raillon C, Granjon P, Graf M, Steinbock LJ, Radenovic A. 2012. Fast and automatic processing of multi-level events in nanopore translocation experiments. *Nanoscale* 4:4916–24
99. Ramsay WJ, Bayley H. 2018. Single-molecule determination of the isomers of D-glucose and D-fructose that bind to boronic acids. *Angew. Chem. Int. Ed.* 57:2841–45
100. Ramsay WJ, Bell NAW, Qing Y, Bayley H. 2018. Single-molecule observation of the intermediates in a catalytic cycle. *J. Am. Chem. Soc.* 140:17538–46

101. Reany O, Romero-Ruiz M, Khurana R, Mondal P, Keinan E, Bayley H. 2024. Stochastic sensing of chloride anions using an α-hemolysin pore with a *semiaza*-bambusuril adapter. *Angew. Chem. Int. Ed.* 63:e202406719
102. Robertson JWF, Reiner JE. 2018. The utility of nanopore technology for protein and peptide sensing. *Proteomics* 18:1800026
103. Sanchez-Quesada J, Ghadiri MR, Bayley H, Braha O. 2000. Cyclic peptides as molecular adapters for a pore-forming protein. *J. Am. Chem. Soc.* 122:11757–66
104. Satheesan R, Janeena A, Mahendran KR. 2025. Hetero-oligomeric protein pores for single-molecule sensing. *J. Membr. Biol.* 258:257–67
105. Shin S-H, Bayley H. 2005. Stepwise growth of a single polymer chain. *J. Am. Chem. Soc.* 127:10462–63
106. Shin S-H, Luchian T, Cheley S, Braha O, Bayley H. 2002. Kinetics of a reversible covalent-bond-forming reaction observed at the single-molecule level. *Angew. Chem. Int. Ed.* 41:3707–9
107. Shin S-H, Steffensen MB, Claridge TDW, Bayley H. 2007. Formation of a chiral center and pyrimidal inversion at the single-molecule level. *Angew. Chem. Int. Ed.* 46:7412–16
108. Song L, Hobaugh MR, Shustak C, Cheley S, Bayley H, Gouaux JE. 1996. Structure of staphylococcal α-hemolysin, a heptameric transmembrane pore. *Science* 274:1859–65
109. Steffensen MB, Rotem D, Bayley H. 2014. Single-molecule analysis of chirality in a multicomponent reaction network. *Nat. Chem.* 6:603–7
110. Su Z, Chen T, Liu X, Kang X. 2025. Size-tunable transmembrane nanopores assembled from decomposable molecular templates. *Biosens. Bioelectron.* 267:116780
111. Sun W, Xiao Y, Wang K, Zhang S, Yao L, et al. 2025. Nanopore discrimination of rare earth elements. *Nat. Nanotechnol.* 20:523–31
112. Tsutsui M, Takaai T, Yokota K, Kawai T, Washio T. 2021. Deep learning-enhanced nanopore sensing of single-nanoparticle translocation dynamics. *Small Methods* 5:2100191
113. Wang K, Yang X, Xiao Y, Cao Z, Zhang S, et al. 2023. Simultaneous identification of major thyroid hormones by a nickel immobilized biological nanopore. *Nano Lett.* 24:305–11
114. Wang K, Yang X, Zhang S, Zhang P, Huang S. 2023. Nanopore discrimination of nucleotide sugars. *Nano Lett.* 23:8620–27
115. Wang K, Zhang S, Zhou X, Yang X, Li X, et al. 2024. Unambiguous discrimination of all 20 proteinogenic amino acids and their modifications by nanopore. *Nat. Methods* 21:92–101
116. Wang L, Brock A, Herberich B, Schultz PG. 2001. Expanding the genetic code of *Escherichia coli*. *Science* 292:498–500
117. Wang L, Xie J, Schultz PG. 2006. Expanding the genetic code. *Annu. Rev. Biophys.* 35:225–49
118. Wang S, Cao J, Jia W, Guo W, Yan S, et al. 2020. Single molecule observation of hard–soft-acid–base (HSAB) interaction in engineered *Mycobacterium smegmatis* porin A (MspA) nanopores. *Chem. Sci.* 11:879–87
119. Wang Y, Fan P, Zhang S, Wang L, Li X, et al. 2022. Discrimination of ribonucleoside mono-, di-, and triphosphates using an engineered nanopore. *ACS Nano* 16:21356–65
120. Wang Y, Guan X, Zhang S, Liu Y, Wang S, et al. 2021. Structural-profiling of low molecular weight RNAs by nanopore trapping/translocation using *Mycobacterium smegmatis* porin A. *Nat. Commun.* 12:3368
121. Wang Y, Zhang S, Jia W, Fan P, Wang L, et al. 2022. Identification of nucleoside monophosphates and their epigenetic modifications using an engineered nanopore. *Nat. Nanotechnol.* 17:976–83
122. Wanunu M. 2012. Nanopores: a journey towards DNA sequencing. *Phys. Life Rev.* 9:125–58
123. Watson JL, Juergens D, Bennett NR, Trippe BL, Yim J, et al. 2023. De novo design of protein structure and function with RFdiffusion. *Nature* 620:1089–100
124. Wei X, Ma D, Ou J, Song G, Guo J, et al. 2024. Narrowing signal distribution by adamantane derivatization for amino acid identification using an α-hemolysin nanopore. *Nano Lett.* 24:1494–501
125. Wen C, Dematties D, Zhang SL. 2021. A guide to signal processing algorithms for nanopore sensors. *ACS Sens.* 6:3536–55
126. Wendell D, Jing P, Geng J, Subramaniam V, Lee TJ, et al. 2009. Translocation of double-stranded DNA through membrane-adapted phi29 motor protein nanopores. *Nat. Nanotechnol.* 4:765–72

127. Wu H-C, Astier Y, Maglia G, Mikhailova E, Bayley H. 2007. Protein nanopores with covalently attached molecular adapters. *J. Am. Chem. Soc.* 129:16142–48
128. Wu X-Y, Li M-Y, Yang S-J, Jiang J, Ying Y-L, et al. 2023. Controlled genetic encoding of unnatural amino acids in a protein nanopore. *Angew. Chem. Int. Ed.* 62:e202300582
129. Wu Y, Gooding JJ. 2022. The application of single molecule nanopore sensing for quantitative analysis. *Chem. Soc. Rev.* 51:3862–85
130. Yamada T, Sugiura H, Mimura H, Kamiya K, Osaki T, Takeuchi S. 2021. Highly sensitive VOC detectors using insect olfactory receptors reconstituted into lipid bilayers. *Sci. Adv.* 7:eabd2013
131. Yan S, Wang L, Du X, Zhang S, Wang S, et al. 2021. Rapid and multiplex preparation of engineered *Mycobacterium smegmatis* porin A (MspA) nanopores for single molecule sensing and sequencing. *Chem. Sci.* 12:9339–46
132. Yang C-N, Liu W, Liu H-T, Zhang J-C, Long Y-T, Ying Y-L. 2025. Electrochemical kinetic fingerprinting of single-molecule coordinations in confined nanopores. *Faraday Discuss.* 257:29–43
133. Yang C-N, Liu W, Liu H-T, Zhang J-C, Yu R-J, et al. 2024. Electrochemical visualization of single-molecule thiol substitution with nanopore measurement. *ACS Meas. Sci. Au* 4:76–80
134. Yang J, Wang K, Zhang S, Zheng X, Cui T, et al. 2023. Site-specific introduction of bioorthogonal handles to nanopores by genetic code expansion. *Angew. Chem. Int. Ed.* 62:e202216115
135. Yang Y, Li Y, Tang L, Li J. 2024. Single-molecule bioelectronic sensors with AI-aided data analysis: convergence and challenges. *Precis. Chem.* 2:518–38
136. Zaitseva E, Obergrussberger A, Weichbrodt C, Boukhet M, Bernhard F, et al. 2021. Electrophysiology on channel-forming proteins in artificial lipid bilayers: next-generation instrumentation for multiple recordings in parallel. In *Patch Clamp Electrophysiology: Methods and Protocols*, ed. M Dallas, D Bell. Humana Press
137. Zhang J, Cao J, Jia W, Zhang S, Yan S, et al. 2021. Mapping potential engineering sites of *Mycobacterium smegmatis* porin A (MspA) to form a nanoreactor. *ACS Sens.* 6:2449–56
138. Zhang M, Tang C, Wang Z, Chen S, Zhang D, et al. 2024. Real-time detection of 20 amino acids and discrimination of pathologically relevant peptides with functionalized nanopore. *Nat. Methods* 21:609–18
139. Zhang S, Cao Z, Fan P, Sun W, Xiao Y, et al. 2023. Discrimination of disaccharide isomers of different glycosidic linkages using a modified MspA nanopore. *Angew. Chem. Int. Ed.* 63:e202316766
140. Zhang S, Cao Z, Fan P, Wang Y, Jia W, et al. 2022. A nanopore-based saccharide sensor. *Angew. Chem. Int. Ed.* 61:e202203769
141. Zhang X, Dou L, Zhang M, Wang Y, Jiang X, et al. 2021. Real-time sensing of neurotransmitters by functionalized nanopores embedded in a single live cell. *Mol. Biomed.* 2:6
142. Zhang Y, Yi Y, Li Z, Zhou K, Liu L, Wu H-C. 2023. Peptide sequencing based on host–guest interaction-assisted nanopore sensing. *Nat. Methods* 21:102–9
143. Zhao C, Wang Y, Chen C, Zhu Y, Miao Z, et al. 2024. Direct and continuous monitoring of multicomponent antibiotic gentamicin in blood at single-molecule resolution. *ACS Nano* 18:9137–49